Experimental realization of a long-lived striped Bose-Einstein condensate induced by momentum-space hopping

Thomas M. Bersano, Junpeng Hou, Sean Mossman, Vandna Gokhroo, Xi-Wang Luo, Kuei Sun, Chuanwei Zhang, and Peter Engels

Phys. Rev. A **99**, 051602 — Published 30 May 2019

DOI: 10.1103/PhysRevA.99.051602

Experimental realization of a long-lived striped Bose-Einstein condensate induced by momentum-space hopping

Thomas M. Bersano,[1] Junpeng Hou,[2] Sean Mossman,[1] Vandna Gokhroo,[1]
Xi-Wang Luo,[2] Kuei Sun,[2] Chuanwei Zhang,[2,*] and Peter Engels[1,†]

[1]*Department of Physics and Astronomy, Washington State University, Pullman, Washington 99164-2814*
[2]*Department of Physics, The University of Texas at Dallas, Richardson, Texas 75080-3021, USA*

The search for supersolid-like phases has attracted great attention in the fields of condensed matter and ultracold atom physics. Here we experimentally demonstrate a route for realizing a superfluid stripe-phase in a spin-orbit coupled Bose-Einstein condensate by employing a weak optical lattice to induce momentum-space hopping between two spin-orbit band minima. We characterize the striped ground state as a function of lattice coupling strength and spin-orbit detuning and find good agreement with mean-field simulations. We observe coherent Rabi oscillations in momentum space between two band minima and demonstrate a long lifetime of the ground state. Our work offers an exciting new and stable experimental platform for exploring superfluid stripe-phases and their exotic excitations, which may shed light on the properties of supersolid-like states.

Introduction. Supersolidity is an exotic phase of matter which simultaneously possesses the crystalline properties of a solid and the unique flow properties of a superfluid [1]. Such simultaneous breaking of continuous translational symmetry and U(1) gauge symmetry was first predicted for solid helium [2, 3], but convincing evidence of a supersolid state in this system has remained elusive [4]. In recent years, the experimental realization of spin-orbit coupling in ultracold atomic gases [5–17] has opened a new pathway for demonstrating long-sought supersolid-like states [18–30].

The lowest energy band in the dispersion of a spin-orbit coupled (SOC) Bose-Einstein condensate (BEC) is characterized by two local minima at distinct momenta [5]. For a narrow range of system parameters, mean-field interactions within a BEC favor a ground state which is composed of a coherent superposition of two plane-wave states at the dispersion minima [22]. This superposition leads to density modulations in real space, or stripes, therefore breaking translational symmetry. Such a stripe-phase was initially proposed for SOC BECs where the pseudospins are defined by two atomic hyperfine states [5], but its experimental realization is challenging due to the sensitivity of the state to magnetic field fluctuations and the weakness of the density modulation. Recent works have attempted to sidestep these difficulties in creative ways, leading to experimental observations of some signatures of superfluid stripe phases in different systems [31–34].

Despite these significant advances, there are experimental challenges such as short lifetime and weak stripe density modulation [32] that may prevent further experimental investigations of supersolid properties of the stripe phase. Therefore the quest for a robust and long-lived platform remains. In this Letter, we show that the superposition of two local band minima to form a supersolid-like ground state can be robustly achieved by means other than atomic interactions. Specifically, we engineer momentum-space hopping between two local band minima in a SOC BEC driven by a weak optical lattice [35–37]. The coupling between different momenta through static or moving optical lattices has been widely used in ultracold atomic gases for engineering versatile types of physics [38–41], but momentum states involved in such coupling schemes are usually not local band minima and thus have short lifetime. Here such a coupling is applied between two local band minima, hence denoted as hopping, in analogy to the hopping between real-space double wells.

When the decrease of the energy due to momentum-state hopping exceeds the increase of the interaction energy due to density modulation, a stripe-phase is more favorable than a plane-wave state at a single dispersion minimum [42]. In a scheme where spin-orbit coupling is induced by Raman coupling between two atomic hyperfine states, this condition can be easily satisfied even for large Raman coupling strengths and detunings, yielding a large parameter region with strong density modulation and spin mixture. While the breaking of continuous translational symmetry is triggered by a weak optical lattice, rather than being spontaneously broken, the resulting stripe-phase shares similar physics with an authentic supersolid state [43]. In this sense, the addition of momentum hopping to a SOC BEC offers a robustly tunable and long-lived experimental platform for exploring exotic superfluid stripe-phase excitations (e.g. breathing modes, roton excitations and collective dynamics [44]), which may shed light on the properties of supersolid-like states that are largely unexplored in experiments.

In our experiments, we first verify that the spin and momentum composition of our experimentally realized state is consistent with the expected ground state stripe-phase. We then probe the coherent momentum hopping between two dispersion minima in the SOC system by suddenly turning on a weak optical lattice to induce Rabi

*Email address: chuanwei.zhang@utdallas
†Email address: engels@wsu.edu

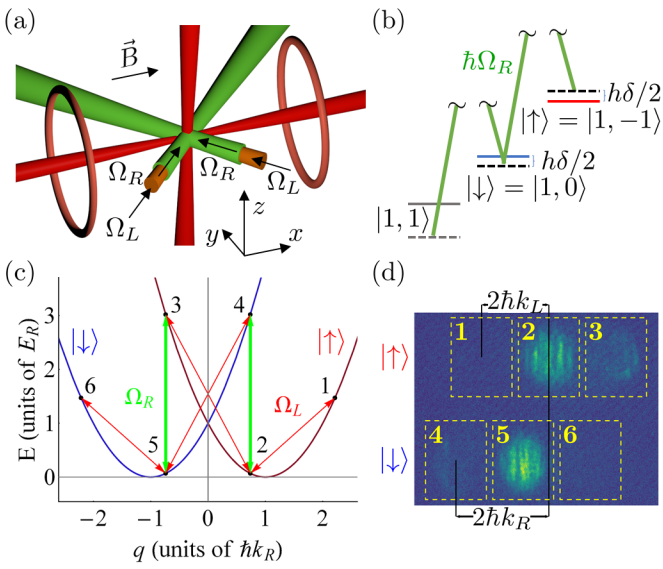

FIG. 1: (a) Schematic of the experimental configuration. A BEC is held in a crossed dipole trap (red) in the presence of a 10 Gauss bias field. A pair of Raman beams (green) collinear with a pair of lattice beams (red) intersect at the BEC position. (b) The Raman coupling scheme. (c) The Raman coupling (green arrows) and the lattice coupling (red arrows) of the relevant momentum states in a rotated spin basis at zero detuning. (d) An example of an experimental measurement using absorption imaging after time-of-flight through a Stern-Gerlach field. The bare states are enumerated to correspond with the marking on the bare-state coupling scheme in (c).

oscillations. Finally, we investigate the coherence and lifetime of the ground state stripe-phase by quenching the spin-orbit detuning at different times and observing ensuing the population dynamics. These experimental observations of ground states properties and dynamics are in good agreement with our numerical simulations of the Gross-Pitaevskii equation (GPE) and therefore provide evidence for the successful production of a stripe-phase ground state.

Spin-orbit coupling with lattice-assisted hopping. We consider the experimental geometry shown in Fig. 1(a). A BEC containing $\approx 2\times10^5$ atoms is prepared in a crossed dipole trap with trapping frequencies $\{\omega_x,\omega_y,\omega_z\} = 2\pi\{33.6, 172, 139\}$ Hz. Two 789 nm Raman beams are incident on the BEC at 45° angles relative to the x-axis, inducing spin-orbit coupling along the x-direction. These Raman beams couple two atomic spin states $|1,-1\rangle$ and $|1,0\rangle$ within the $F=1$ hyperfine manifold, which we will refer to as pseudospin $|\uparrow\rangle$ and $|\downarrow\rangle$ respectively, as shown in Fig. 1(b). This two-photon Raman transition is detuned by δ, while the third spin state ($|1,1\rangle$) is shifted far out of resonance by the quadratic Zeeman shift in a 10 G bias field, leaving it effectively decoupled from the other two states.

The coupled spin states are separated in momentum space by $2\hbar k_R$ where the Raman recoil momentum $\hbar k_R$ is the wavevector of the Raman beams projected onto the x-axis. In a rotated basis, the states are described by a quasi-momentum given by $q = p \pm \hbar k_R$ for the two spin states, where p is the free-particle momentum. The spin-orbit coupling can then be visualized as vertical transitions (green) in Fig. 1(c). Diagonalization of the SOC Hamiltonian results in a two-band structure where, for suitable parameters, the lower spin-orbit band features two minima that are located at $q_{\min} = \pm\hbar k_R\sqrt{1-(\frac{\hbar\Omega_R}{4E_R})^2}$ in single-particle regimes [22]. Here $\hbar\Omega_R$ represents the Raman coupling strength, the recoil energy is $E_R = \hbar^2k_R^2/2m$, and m is the atomic mass of ^{87}Rb.

In addition to the Raman beams, two 1064 nm lattice beams copropagating with the Raman beams create an optical lattice potential $V_L = 2\hbar\Omega_L\sin^2(k_Lx)$ along the x-direction. This static spin-independent lattice can provide a $2\hbar k_L$ momentum-kick while conserving the spin [42]. This is illustrated by the diagonal couplings (red) marked in Fig. 1(c). The key feature of this configuration is that the wavelength of the lattice beams and the Raman coupling strength are chosen such that the lattice couples the two minima of the lower spin-orbit band, i.e. $\hbar k_L = |q_{\min}|$.

The dynamics of this system can be described by a one-dimensional GPE under the mean-field approximation,

$$i\hbar\frac{\partial}{\partial t}\psi = \left(H_{\rm SOC} + V_L + \frac{1}{2}m\omega_x^2x^2 + \frac{g}{2}|\psi|^2\right)\psi, \quad (1)$$

where ω_x is the trapping frequency along x and $\psi = (\psi_\uparrow, \psi_\downarrow)^T$ is the two-component spinor wavefunction normalized by the total particle number $N = \int dx\psi^\dagger\psi$. The spin-orbit coupling term is

$$H_{\rm SOC} = \begin{pmatrix} \frac{1}{2m}(q_x-\hbar k_R)^2 - \frac{\hbar\delta}{2} & \frac{1}{2}\hbar\Omega_R \\ \frac{1}{2}\hbar\Omega_R & \frac{1}{2m}(q_x+\hbar k_R)^2 + \frac{\hbar\delta}{2} \end{pmatrix}. \quad (2)$$

Although it is not obvious in the bare momentum basis, the two spin-orbit band minima are directly coupled in the SOC dressed basis by the weak optical lattice [42], which we name as "*momentum-space hopping*".

Ground-state phase diagram. The momentum space hopping gives rise to strong density modulations in real-space (a typical real space density profile is provided in the supplementary material [42]) resulting from a coherent population of both band minima at quasimomenta $\pm\hbar k_L$. In the absence of spin-orbit coupling, such high density modulation would usually be achieved in deep optical lattices with lattice depths $\hbar\Omega_L \gtrsim 10E_R$, while here $\hbar\Omega_L \approx E_R$ and the strong modulation mainly originates from large Raman coupling [42]. Given the separation of the momentum minima $2q_{\min}$, the real-space distance between the modulation peaks is $\pi/q_{\min} = 0.76$ μm, which is confirmed in the GPE simulations. Experimentally, we cannot directly observe density modulations at this length scale due to the optical resolution limit of

our imaging configuration. Instead, we reconstruct the ground state wavefunction from observable parameters, such as the momentum space distribution and spin polarization of the ground state, and ensure coherence and superfluidity by demonstrating coherent Rabi oscillations.

We begin by exploring the momentum space distribution and spin polarization of the ground state as a function of lattice coupling strength $\hbar\Omega_L$ and spin-orbit detuning δ. After adiabatically dressing the BEC with spin-orbit coupling at a large detuning $\delta = 5$ kHz, the lattice beams are ramped on over 50 ms and then the Raman detuning is adiabatically lowered to a final value. The momentum distribution of each spin in the resulting ground state is measured through Stern-Gerlach imaging after expansion such that the momentum states separate horizontally, while the spin states separate vertically, as shown in Fig. 1(d). The total spin-polarization of the system is given by $\sigma_z = \sum_i s_i N_i / \sum_i |s_i| N_i$, where N_i is the number of atoms in the undressed state i, as marked in Fig. 1, with pseudo-spin s_i, which we take to be $1/2$ and $-1/2$ for atoms in hyperfine levels $|1,-1\rangle$ $(i = 1,2,3)$ and $|1,0\rangle$ $(i = 4,5,6)$ respectively. The experimental data are presented along with the results from numerical simulations in Fig. 2.

In Fig. 2(a), we plot the fractional populations, $\rho_i = N_i/N$, of atoms which contribute to the two local band minima $\pm q_{\min}$ for each spin state as a function of $\hbar\Omega_L$ for $\delta = 250$ Hz. The simultaneous occupation of $\pm q_{\min}$ for spin up (down) indicates the existence of a stripe density modulation $\propto \left|\rho_{2(4)}^{1/2} e^{iq_{\min}x} + \rho_{3(5)}^{1/2} e^{-iq_{\min}x}\right|^2$ [42] with the modulation amplitude $\propto \left|\rho_{2(4)}\rho_{3(5)}\right|^{1/2}$. The numerically determined ground state phase diagram as a function of spin-orbit detuning and lattice strength, shown in Fig. 2(b), reveals that for small ratios of $|\hbar\Omega_L/\delta|$, nearly all atoms occupy one spin state. As the ratio increases, the two band minima become more evenly populated and the spin-polarization approaches zero. Intuitively, we see a finite spin-orbit detuning energetically favors one spin-state while the lattice coupling mixes the spin-momentum states. A closer observation reveals that the spin polarization changes smoothly (a crossover) with respect to detuning when the lattice coupling is strong (Fig. 2(d-f)), but shows an abrupt change (a first order phase transition) when the coupling is weak (Fig. 2(c)). This result is due to the competition between interatomic interaction and lattice coupling [37]. Further discussion of the ground state phase diagram can be found in the supplement. The experimentally determined spin-polarizations are in excellent, quantitative agreement with numerical values (Fig. 2(c-f)), indicating that the physically realized system is consistent with the spin-momentum mixtures which result in the superfluid stripe-phase observed in the numerics.

Coherent Rabi oscillation. The coherent nature of the lattice-induced hopping between the two band minima can be experimentally demonstrated by observing Rabi

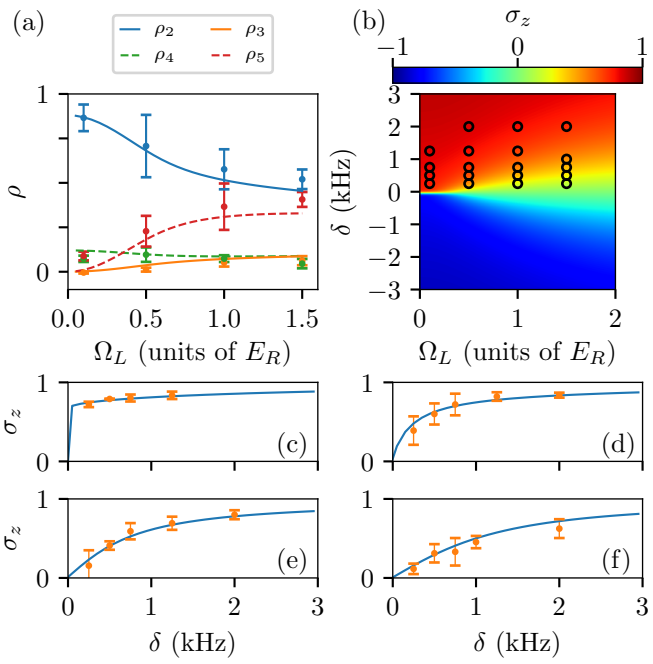

FIG. 2: (a) Fractional bare state populations of the dressed ground state as a function of Ω_L for $\delta = 250$ Hz. (b) Numerical simulation of the ground state spin-polarization phase diagram as a function of δ and Ω_L. The circles indicate the locations experimentally probed in the following subfigures. (c)-(f) Experimental data (dots) and numerical prediction (lines) of spin polarization as a function of Raman detuning for $\Omega_L = 0.1$(c), 0.5(d), 1.0(e), and 1.5 E_R(f) respectively. All numerics and experiments are done with spin-orbit coupling strength $\hbar\Omega_R = 2.7E_R$. In all figures, experimental data points are averages over four measurements with error bars given by statistical error.

oscillations induced by a sudden quench of system parameters. After adiabatically dressing the BEC with spin-orbit coupling, the lattice beams are suddenly turned on, which initiates an oscillation between the two spin-orbit dispersion minima. After a chosen evolution time, all beams are turned off and the individual spin/momentum states are imaged. The resulting spin polarization oscillates in time as shown in Fig. 3(a). The observed oscillation frequency is in good agreement with the GPE simulation, demonstrating the coherent dynamics of the system. Additionally, Fig. 3(b) shows the same oscillation for particular spin-momentum state pairs as marked in Fig. 1(d), where $\sigma_{ij} = (N_i - N_j)/(N_i + N_j)$. We see good agreement between the experimental values for each of the dominant spin-momentum coupling channels and the corresponding GPE simulation. While the vast majority of the atoms populate the bare states marked 2 and 5, Fig. 3(b) indicates that we are able to observe and resolve the coherent oscillations in the coupled spin-momentum space beyond simple spin-orbit coupling, in agreement with GPE simulation.

To explore the role of particle interactions, Fig. 3(a)

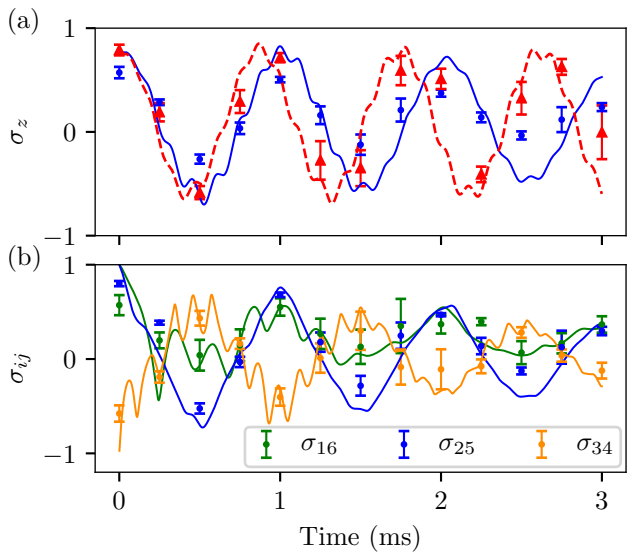

FIG. 3: (a) The Rabi oscillation of the total spin polarization after suddenly jumping on the lattice. Experimental measurements are given by blue and red points, for an average of 2.4×10^5 and 0.9×10^5 atoms, respectively. Blue solid and red dashed lines represent numerical simulations with and without interactions, respectively. (b) The Rabi oscillations between individual spin-momentum channels corresponding to the bare-state basis as marked in Fig. 1(d). The data shown here correspond to $\hbar\Omega_R = 2.7E_R$, $\delta = 250$ Hz and $\hbar\Omega_L = 1.0E_R$.

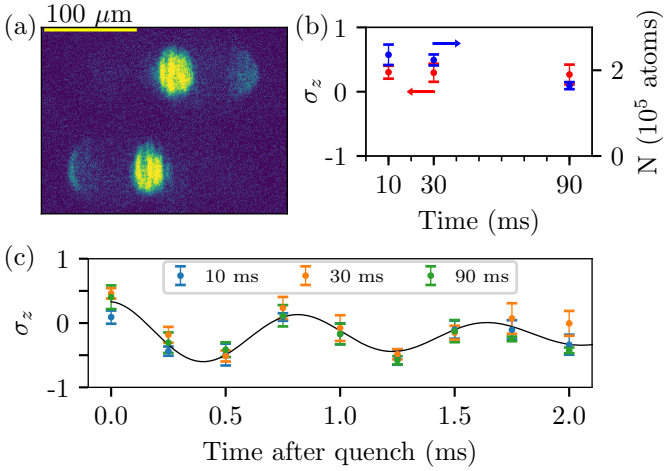

FIG. 4: (a) A composite of four time-of-flight images after 10 ms holding in the ground state (before quench). (b) Plot of the spin-polarization (red) and atom numbers (blue) after different holding time. (c) Detuning quench induced oscillations. A least-squares fit to a damped harmonic oscillation is shown as a guide to the eye. $\hbar\Omega_R = 2.7E_R$ and $\hbar\Omega_L = 1.0E_R$.

shows the results of GPE simulations with and without interactions. A two-level single-particle Rabi oscillation has a frequency given by $\hbar\omega = \sqrt{(\hbar\delta k_L/2k_R)^2 + \tilde{V}^2}$ where $\tilde{V} = \hbar\Omega_L\sqrt{1-(k_L/k_R)^2}/2$ is the effective coupling strength [42]. With the experimental parameters described in Fig. 3, the single-particle Rabi oscillation period is evaluated to be 0.8 ms, which is consistent with GPE simulation without interaction. The role played by nonlinear effects from interatomic interaction is treated on the mean-field level through a variational method [42]. Intuitively, the density-density interaction, which dominates over spin interaction in ^{87}Rb, costs energy and thus makes it less favorable for the condensate to simultaneously occupy both momentum states. As a result, we expect the interactions to reduce the frequency of oscillation and introduce damping effects, which are confirmed by our GPE simulations. We observe strong agreement between numerical simulations with interactions and experimental observations, though the experimental data exhibit stronger damping which is not captured by the mean-field analysis. Some higher frequency, lower amplitude oscillations apparent in both single-particle and interacting cases in Fig. 3 are signatures of highly detuned couplings within the SOC dressed states. Those high-energy states are coupled with different coupling strengths and are less populated, leading to the small ripples on the overall Rabi oscillation. The Rabi oscillations shown here are driven by a weak lattice which is slightly stronger than the mean field interaction strength. This character is indicative of the dynamics underlying momentum-space Josephson effects [37], which is beyond the scope of these experimental observations.

Stripe-phase ground state stability. While the arguments given above have indicated that we reliably prepare the appropriate spin-momentum mixtures to achieve a high-contrast stripe-phase, those mixtures must be coherent over a long period of time to produce the expected density modulation for further investigation of dynamical properties and excitations of superfluid stripe phases. To study the coherent lifetime of the ground stripe state, we prepare the ground state and then initiate quenches after various wait times. The reproducibility of the ground-state quench dynamics provides evidence for the long time phase stability of the spin-momentum mixtures which produces the stripe-phase. When a ground-state system is quenched, the behavior following the quench is consistent regardless of when the quench takes place. However, if a system is not in a ground state, that system is dynamic and the behavior following the quench depends on when the quench occurs.

An example of such a quench is a sudden jump of the spin-orbit detuning δ, which induces coherent oscillations of the spin polarization and corresponding momentum states. We begin by preparing the superfluid stripe-phase as described earlier and quench δ from 500 Hz to -500 Hz. We perform the quench 10, 30, or 90 ms after the preparation of the ground state and in all cases observe subsequent oscillations of similar amplitude and frequency. Fig. 4(a) shows the time-of-flight image after 10 ms of holding the ground state, which clearly shows the scarcity of thermal atoms and correspondingly

high condensate fraction. In Fig. 4(b), we plot the spin-polarizations and condensate atom numbers versus different holding times before the quench. The spin polarization does not change with time and the decay of the atom number is attributed to the heating from the Raman lasers. Fig. 4(c) shows the evolution of the spin-polarization after each of the wait times along with a best-fit curve as a guide to the eye. While the condensate loses atoms as it is held in the striped ground state at a similar rate to a SOC BEC, the consistency of the quench dynamics indicates that the ground state supported by the lattice-coupled SOC system is stable in phase for times on the order of at least 100 ms. This opens up the possibility to investigate long-time dynamics of supersolid-like phases.

Conclusions. In this work, we have demonstrated a robust framework for the production of a high-contrast, long-lived, and tunable ground state stripe-phase in a SOC BEC. By showing quantitative agreement with numerical simulations of the GPE, we have demonstrated that our experimental configuration is able to reliably produce the expected stripe-phase over a broad parameter space. We confirm that the experimental momentum and spin distributions agree with those expected for both the static and dynamic cases and are coherent over long times (∼100 ms).

The application of optical lattice driven momentum-space hopping allows for the SOC stripe-phase to exist over a broad parameter space comparing to previous experiments. Therefore, this configuration opens up new possibilities for investigations of excitation dynamics such as roton modes and breathing modes as well as studies of defects or barriers passing through the superfluid stripe-phase. These studies will shed light of supersolid properites of superfluid stripes, which are largely unexplored in experiments. Additionally, we note that such a setup can also be used to realize momentum-space Josephson effects when the lattice coupling strength is weak compared to particle interactions [37].

Acknowledgements. TMB, SM, VG and PE acknowledge funding from the NSF (PHY-1607495). JH, XL, KS, and CZ are thankful for support from NSF (PHY-1505496), AFOSR (FA9550-16-1-0387) and ARO (W911NF-17-1-0128).

[1] M. Boninsegni and N. V. Prokofv, Supersolids: What and where are they? Rev. Mod. Phys. **84**, 759 (2012).
[2] D.J Thouless, The flow of a dense superfluid, Ann. Phys. **52**, 403 (1971).
[3] A. F. Andreev and I. M. Lifshitz, Quantum Theory of Defects in Crystals, Sov. Phys. JETP **29**, 1107 (1971).
[4] Duk Y. Kim and Moses H. W. Chan, Absence of Supersolidity in Solid Helium in Porous Vycor Glass, Phys. Rev. Lett. **109**, 109 (2012).
[5] Y.-J. Lin, K. Jiménez-García, and I. B. Spielman, Spin-orbit-coupled Bose-Einstein condensates, Nature (London) **471**, 83 (2011).
[6] Jin-Yi Zhang, Si-Cong Ji, Zhu Chen, Long Zhang, Zhi-Dong Du, Bo Yan, Ge-Sheng Pan, Bo Zhao, You-Jin Deng, Hui Zhai, Shuai Chen, and Jian-Wei Pan, Collective Dipole Oscillations of a Spin-Orbit Coupled Bose-Einstein Condensate, Phys. Rev. Lett. **109**, 115301 (2012).
[7] C. Qu, C. Hamner, M. Gong, C. Zhang, and P. Engels, Observation of Zitterbewegung in a spin-orbit-coupled Bose-Einstein condensate, Phys. Rev. A **88**, 021604(R) (2013).
[8] A. J. Olson, S.-J. Wang, R. J. Niffenegger, C.-H. Li, C. H. Greene, and Y. P. Chen, Tunable Landau-Zener transitions in a spin-orbit-coupled Bose-Einstein condensate, Phys. Rev. A **90**, 013616 (2014).
[9] C. Hamner, C. Qu, Y. Zhang, J. Chang, M. Gong, C. Zhang, and P. Engels, Dicke-type phase transition in a spin-orbit-coupled Bose-Einstein condensate, Nat. Commun. **5**, 4023 (2014).
[10] P. Wang, Z.-Q. Yu, Z. Fu, J. Miao, L. Huang, S. Chai, H. Zhai, and J. Zhang, Spin-Orbit Coupled Degenerate Fermi Gases, Phys. Rev. Lett. **109**, 095301 (2012).
[11] L. W. Cheuk, A. T. Sommer, Z. Hadzibabic, T. Yefsah, W. S. Bakr, and M. W. Zwierlein, Spin-Injection Spectroscopy of a Spin-Orbit Coupled Fermi Gas, Phys. Rev. Lett. **109**, 095302 (2012).
[12] R. A. Williams, M. C. Beeler, L. J. LeBlanc, K. Jiménez-García, and I. B. Spielman, Raman-Induced Interactions in a Single-Component Fermi Gas Near an *s*-Wave Feshbach Resonance, Phys. Rev. Lett. **111**, 095301 (2013).
[13] N. Q. Burdick, Y. Tang, and B. L. Lev, Long-Lived Spin-Orbit-Coupled Degenerate Dipolar Fermi Gas, Phys. Rev. X **6**, 031022 (2016).
[14] B. Song, C. He, S. Zhang, E. Hajiyev, W. Huang, X.-J. Liu, and G.-B. Jo, Spin-orbit-coupled two-electron Fermi gases of ytterbium atoms, Phys. Rev. A **94**, 061604(R) (2016).
[15] L. Huang, Z. Meng, P. Wang, P. Peng, S.-L. Zhang, L. Chen, D. Li, Q. Zhou & J. Zhang, Experimental realization of two-dimensional synthetic spin–orbit coupling in ultracold Fermi gases, Nat. Phys. **12**, 540 (2016).
[16] Zengming Meng, Lianghui Huang, Peng Peng, Donghao Li, Liangchao Chen, Yong Xu, Chuanwei Zhang, Pengjun Wang, and Jing Zhang, Experimental Observation of a Topological Band Gap Opening in Ultracold Fermi Gases with Two-Dimensional Spin-Orbit Coupling, Phys. Rev. Lett. **117**, 235304 (2016).
[17] Z. Wu, L. Zhang, W. Sun, X.-T. Xu, B.-Z. Wang, S.-C. Ji, Y. Deng, S. Chen, X.-J. Liu, J.-W. Pan, Realization of two-dimensional spin-orbit coupling for Bose-Einstein condensates, Science **354**, 83 (2016).
[18] T. D. Stanescu, B. Anderson, and V. Galitski, Spin-orbit coupled Bose-Einstein condensates, Phys. Rev. A **78**, 023616 (2008).
[19] C. Wu, I. Mondragon-Shem, and X.-F. Zhou, Unconventional Bose-Einstein Condensations from Spin-Orbit Coupling, Chin. Phys. Lett. **28**, 097102 (2011).
[20] C. Wang, C. Gao, C.-M. Jian, and H. Zhai, Spin-orbit coupled spinor Bose-Einstein condensates, Phys. Rev.

Lett. **105**, 160403 (2010).
[21] T.-L. Ho and S. Zhang, Bose-Einstein condensates with spin-orbit interaction, Phys. Rev. Lett. **107**, 150403 (2011).
[22] Y. Li, L. Pitaevskii, and S. Stringari, Quantum tricriticality and phase transitions in spin-orbit coupled Bose-Einstein condensates, Phys. Rev. Lett. **108**, 225301 (2012).
[23] Y. Zhang, L. Mao, and C. Zhang, Mean-field dynamics of spin-orbit coupled Bose-Einstein condensates, Phys. Rev. Lett. **108**, 035302 (2012).
[24] H. Hu, B. Ramachandhran, H. Pu, and X.-J. Liu, Spin-orbit coupled weakly interacting Bose-Einstein condensates in harmonic traps, Phys. Rev. Lett. **108**, 010402 (2012).
[25] T. Ozawa and G. Baym, Stability of ultracold atomic bose condensates with rashba spin-orbit coupling against quantum and thermal fluctuations, Phys. Rev. Lett. **109**, 025301 (2012).
[26] K. Sun, C. Qu, Y. Xu, Y. Zhang, and C. Zhang, Interacting spin-orbit-coupled spin-1 Bose-Einstein condensates, Phys. Rev. A **93**, 023615 (2016).
[27] Z.-Q. Yu, Phase transitions and elementary excitations in spin-1 Bose gases with Raman-induced spin-orbit coupling, Phys. Rev. A **93**, 033648 (2016).
[28] G. Martone, F. Pepe, P. Facchi, S. Pascazio, and S. Stringari, Tricriticalities and quantum phases in spin-orbit-coupled spin-1 bose gases, Phys. Rev. Lett. **117**, 125301 (2016).
[29] X.-W. Luo, K. Sun, C. Zhang, Spin-tensor–momentum-coupled Bose-Einstein condensates, Phys. Rev. Lett. **119**, 193001 (2017).
[30] J. Hou, H. Hu, K. Sun, and C. Zhang, Superfluid-Quasicrystal in a Bose-Einstein Condensate, Phys. Rev. Lett. **120**, 060407 (2018).
[31] J. Li, W. Huang, B. Shteynas, S. Burchesky, F. Top, E. Su, J. Lee, A. O. Jamison, and W. Ketterle, Spin-Orbit Coupling and Spin Textures in Optical Superlattices, Phy. Rev. Lett. **117**, 185301 (2016).
[32] J.-R. Li, J. Lee, W. Huang, S. Burchesky, B. Shteynas, F. Ç. Top, A. O. Jamison, and W. Ketterle, A stripe phase with supersolid properties in spin-orbit-coupled Bose-Einstein condensates, Nature (London) **543**, 91 (2017).
[33] J. Léonard, A. Morales, P. Zupancic, T. Esslinger & T. Donner , Supersolid formation in a quantum gas breaking a continuous translational symmetry, Nature (London) **543**, 87 (2017).
[34] L. Chomaz et al, Observation of roton mode population in a dipolar quantum gas, Nat. Phys. **14**, 442 (2018).
[35] G. I. Martone, T. Ozawa, C. Qu, and S. Stringari, Optical-lattice-assisted magnetic phase transition in a spin-orbit-coupled Bose-Einstein condensate, Phys. Rev. A **94**, 043629 (2016).
[36] T. F. J. Poon and X.-J. Liu, Quantum spin dynamics in a spin-orbit-coupled Bose-Einstein condensate, Phys. Rev. A **93**, 063420 (2016).
[37] J. Hou, X.-W. Luo, K. Sun, T. Bersano, V. Gokhroo, S. Mossman, P. Engels, and C. Zhang, Momentum-Space Josephson Effects, Phys. Rev. Lett. **120**, 120401 (2018).
[38] M. F. Andersen, C. Ryu, Pierre Cladé, Vasant Natarajan, A. Vaziri, K. Helmerson, and W. D. Phillips, Quantized Rotation of Atoms from Photons with Orbital Angular Momentum, Rev. Lett. **97**, 170406 (2006).
[39] M. A. Khamehchi, C. Qu, M. E. Mossman, C. Zhang, P. Engels, Spin-momentum coupled Bose-Einstein condensates with lattice band pseudospins, Nat. Commun. **7**, 10867 (2016).
[40] E. J. Meier, F. A. An & B. Gadway, Observation of the topological soliton state in the Su-Schrieffer-Heeger model, Nat. Commun. **7**, 13986 (2016).
[41] F. A. An, E. J. Meier, J. Ang'ong'a, and B. Gadway, Correlated Dynamics in a Synthetic Lattice of Momentum States, Phys. Rev. Lett. **120**, 040407 (2018).
[42] See Supplementary Materials for more details.
[43] G. I. Martone, Quantum Phases and Collective Excitations of a Spin-Orbit-Coupled Bose-Einstein Condensate in a One-Dimensional Optical Lattice, J. Low Temp. Phys. **189**, 262 (2017).
[44] Z. Chen and H. Zhai, Collective-mode dynamics in a spin-orbit-coupled Bose-Einstein condensate, Phys. Rev. A **86**, 041604(R) (2012).